# Neutron scattering study of the competing magnetic correlations in $La_{0.85}Sr_{0.15}CoO_3$

D. Phelan,[1,2] Despina Louca,[1] S. N. Ancona,[3] S. Rosenkranz,[3] H. Zheng,[3] and J. F. Mitchell[3]
[1]*Department of Physics, University of Virginia, Charlottesville, Virginia 22904, USA*
[2]*NIST Center for Neutron Research, National Institute of Standards and Technology, Gaithersburg, Maryland 20899, USA*
[3]*Materials Science Division, Argonne National Laboratory, Argonne, Illinois 60439, USA*
(Received 9 September 2008; revised manuscript received 24 December 2008; published 20 March 2009)

The nature of the competing ferromagnetic and incommensurate spin correlations in the spin-glass phase of $La_{0.85}Sr_{0.15}CoO_3$ has been investigated by various neutron scattering techniques. Spin-polarized scattering indicates that the observed incommensurate peaks are dominantly magnetic in nature. Magnetic field experiments show that a field applied perpendicular to the short-range ordering wave vector destroys the incommensurate correlations and induces long-range ferromagnetic order. However, even for fields up to 7 T, short-range ferromagnetic correlations still coexist with the long-range ordered regions.

DOI: 10.1103/PhysRevB.79.094420 PACS number(s): 75.50.Lk

## I. INTRODUCTION

In transition-metal-oxide materials, competing interactions can lead to phase separation in which several phases coexist inhomogenously in a crystal. Such phase separation may play an important role in the physics of technologically interesting systems, as in the colossal magnetoresistive manganites,[1–4] and determining how phase separation arises and how the competing phases depend on tunable parameters such as pressure or magnetic field is important. Over the past several years, a number of works have highlighted the perovskite cobaltite series, $La_{1-x}Sr_xCoO_3$ (LSCO), as a system with which the phenomena of magnetic phase separation and magnetic inhomogeneities may be studied.[5–9]

The ground state of the parent compound of LSCO, $LaCoO_3$, is a nonmagnetic insulator ($Co^{3+}$ has an $S=0$ ground state in the parent compound). However, as holes are doped into the system by the chemical substitution of $Sr^{2+}$ for $La^{3+}$ ions, static magnetic correlations arising from interactions between $Co^{3+}$ and $Co^{4+}$ ions develop at low temperatures and the conductivity increases. For $x>0.18$, the system becomes metallic, and the magnetic state is described as either a ferromagnet or a ferromagnetic cluster glass.[10,11] For samples with $x<0.18$, the bulk ground state appears to be spin-glass-like:[10,11] a clear divergence is observed between the field-cooled (FC) and zero-field-cooled (ZFC) magnetic susceptibilities, and a distinct aging effect has been observed.[10] Several experimental techniques, such as NMR,[5–7] small-angle neutron scattering (SANS),[8] and single-crystal neutron diffraction,[12] have further characterized the "glassy" state as an inhomogenous phase-separated state in which hole-rich ferromagnetic clusters are embedded in a hole-poor nonferromagnetic matrix. Leighton *et al.*[13] recently deduced that magnetic inhomogeneities persist over the doping range of $0.04<x<0.22$ through SANS and specific-heat measurements of single crystals.

The nonferromagnetic spin correlations in the matrix surrounding the ferromagnetic clusters have been insufficiently understood. Recently, we observed a static, short-ranged, and incommensurate magnetic phase in our single-crystal elastic neutron scattering measurements for compositions between $x=0.05$ and $x=0.20$,[9] and we believe that this observation is a critical piece of the puzzle for understanding the magnetic phase separation in LSCO. In order to further characterize the spin correlations (both ferromagnetic and incommensurate), we have instigated several neutron scattering experiments performed on a single crystal of $La_{0.85}Sr_{0.15}CoO_3$ using polarization analysis and measuring scattering under applied magnetic field. The $La_{0.85}Sr_{0.15}CoO_3$ single crystal exhibits both ferromagnetic and incommensurate neutron scattering intensities.[9] The diffuse ferromagnetic intensity gradually increases as the temperature is lowered below 100 K with an inflection at $T\approx 65$ K ($T_c$). The incommensurate peak, which has a characteristic wave vector of approximately (0.3,0.3,0.3), gradually appears below 90 K with an inflection at $\approx 55$ K ($T_{IC}$). In the present work, we find that the incommensurate intensity is dominantly magnetic, and that under the application of a field the incommensurate intensity is reduced in the (*hhl*) plane. On the other hand, we observe that the ferromagnetic clusters coalesce to form much larger ferromagnetic entities under an applied field, but that some short-range ferromagnetic clusters still remain at fields up to 7 T. The rest of this paper is organized as follows. In Sec. II, the details of the neutron scattering experiments are described. The measurements of the spin-polarized scattering and the field dependence are discussed in Secs. III A and III B, respectively.

## II. EXPERIMENT

The single crystal of $La_{0.85}Sr_{0.15}CoO_3$ is the same one studied in Refs. 12 and 9. The $x=0.15$ composition was chosen because it exhibits the strongest measured incommensurate signal in LSCO (Ref. 9) and, since it lies on the spin-glass side of the magnetic phase diagram, it is less likely to be physically moved by a strong field during the experiment. The single crystal is a twinned trigonally distorted perovskite with space group $R\bar{3}c$. However, for all of the experiments, the sample is aligned in the pseudocubic (*hhl*) zone, and pseudocubic notation is used to describe the diffraction data with the scattering wave vector, $\vec{Q}$, denoted in reciprocal lattice units (rlu).

The measurements in applied magnetic field were performed on the thermal triple-axis spectrometer, BT9, located

 ©2009 The American Physical Society

at the NIST Center for Neutron Research (NCNR), in a 7 T vertical-field superconducting magnet. The field was oriented out of the scattering plane along the $[1,\bar{1},0]$ crystal axis. Two different experimental configurations were used, both with an incident neutron energy of 14.7 meV. For scans along $[h,h,h]$ through the incommensurate magnetic peak, the instrument was operated in three-axis mode, in which a conventional, flat, and highly oriented pyrolytic graphite (HOPG) (002) analyzer was used to select the scattered neutron energy. The horizontal angular collimation of the beam was set to $40'-47'-40'-80'$. Pyrolytic graphite (PG) filters were placed in the incident and scattered beams to filter out higher-energy harmonics. In this case, since the energy transfer was fixed to be zero, elastic scattering was measured within the energy resolution of the instrument, which is approximately 0.4 meV full width at half maximum (FWHM). Scans along [0,0,*l*], which were taken to explore the instantaneous ferromagnetic correlations, were made using a second configuration in which the spectrometer was operated in two-axis mode, whereby the energy analyzer was removed from the scattered beam. In this case, the collimation of the beam was set to $40'-23'-20'$ and a PG filter was placed in the incident beam, but not in the scattered beam, so that the energy-integrated intensity, and hence the instantaneous correlation function, was measured.

The $Q$ dependence of the incommensurate peak intensity was measured on the triple-axis spectrometer, SPINS, located at the NCNR. A thermal incident neutron energy of 14.7 meV was selected by the (004) reflection from an HOPG monochromator and the (002) reflection from an analyzer consisting of three HOPG blades in a conventional flat configuration. One pyrolytic graphite filter was placed in the incident beam.

Spin-polarized measurements, in which spin-flip (SF) and non-spin-flip (NSF) cross sections were determined, were performed to distinguish between nuclear and magnetic origins of neutron scattering intensities. All coherent nuclear scattering is NSF, which means that if a peak is observed in the SF channel, it must have a magnetic component. Note that this case does not preclude the possibility of a nuclear component to the intensity if scattering is also observed in the NSF channel.[14] The spin-polarized measurements were made on the cold-neutron polarized reflectometer, NG1, at the NCNR. The reflectometer was operated as a two-axis diffractometer with a fixed incident energy of 3.626 meV and a Be filter. Fe/Si supermirrors were used as the spin polarizer and analyzer. In this setup, the neutron spin was polarized in the vertical direction, which was out of the scattering plane and along the $(1,\bar{1},0)$ crystal axis. Due to the physical limitation of the maximum scattering angle and the fixed incident energy, the (1,1,0) Bragg peak could not be reached when aligning the sample in the (*hhl*) scattering plane. Only the tilt along (0,0,1) was adjusted. We estimate that the crystal was aligned within 2° along the (1,1,0) arc based on its prior alignment on BT9; however, due to this limitation, the sample was slightly misaligned out of the (*hhl*) plane. Nevertheless, it is safe to compare the NSF to the SF intensity. If the initial polarization is in the up (↑) direction, then $I_{\mathrm{NSF}}(\vec{Q})$ and $I_{\mathrm{SF}}(\vec{Q})$ were measured as the up-up ↑↑ and up-down ↓↑

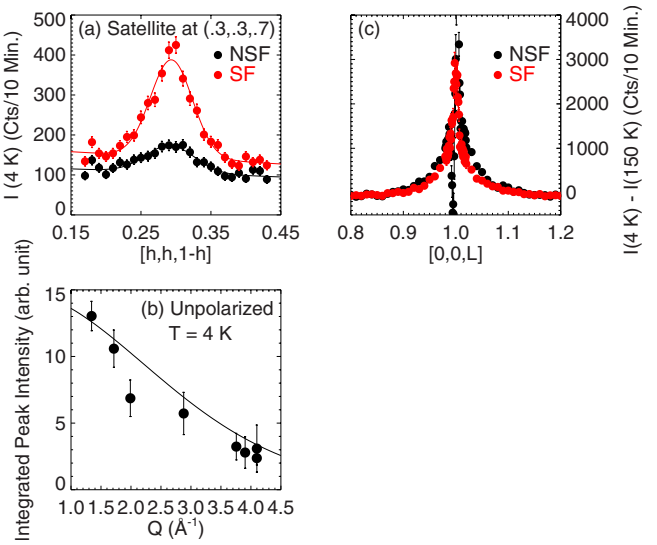


FIG. 1. (Color online) (a) Intensity at the incommensurate reflection (0.3,0.3,0.7) measured in the SF and NSF channels at 4 K. (b) Comparison of the $Q$ dependence of incommensurate reflections (circles) to the square of the magnetic form factor (solid line). (c) $I(4\ \mathrm{K})-I(150\ \mathrm{K})$ measured in the SF and NSF channels for the broad ferromagnetic scattering around (0,0,1). There is some subtracted intensity that falls outside of the data range shown which comes from the change in the lattice constant. Note that the error bars in figures which display raw intensity represent a statistical uncertainty of $\pm 1\sigma$ and the error bars of fitted values in figures (i.e., integrated intensities) represent the $1\sigma$ errors as determined from the covariance matrix.

cross sections, respectively. A flipping ratio of 9.2 was determined from the ratio of $I_{\mathrm{NSF}}/I_{\mathrm{SF}}$ at (0,0,1) at 150 K (nuclear intensity only), well above the spin-glass transition temperature.

## III. RESULTS AND DISCUSSION

### A. Magnetic versus nonmagnetic scattering

Spin-polarized measurements were made to verify the magnetic nature of the incommensurate peak. The SF and NSF intensities measured at the incommensurate peak at $\vec{Q} \approx (0.3,0.3,0.7)$ at $T=4$ K are shown in Fig. 1(a). It can be seen that $I_{\mathrm{SF}} \gg I_{\mathrm{NSF}}$ ($I_{\mathrm{SF}}/I_{\mathrm{NSF}} \approx 3.1$), which proves that the scattering is dominantly magnetic at the incommensurate reflection. Since there is intensity in the NSF channel, the measurement does not rule out a weak nuclear contribution to the incommensurate peak, but we can say that the magnetic intensity is much stronger than any possible nuclear contribution.

Further evidence of the magnetic nature of the incommensurate peaks comes from the $Q$ dependence of the intensity. Since magnetic scattering is proportional to the square of a magnetic form factor which decreases rather quickly with $|\vec{Q}|$, the measured intensity of magnetic peaks should also decrease with increasing $|\vec{Q}|$. On the other hand, nuclear scattering is not constrained by this form factor, and thus following the $|\vec{Q}|$ dependence of the incommensurate peaks can

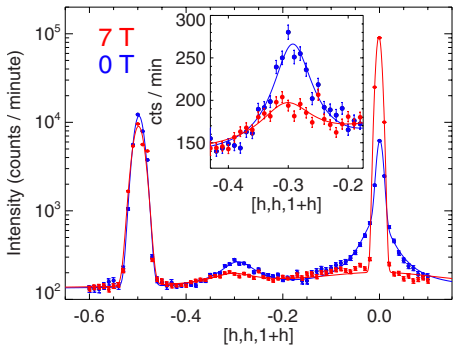


FIG. 2. (Color online) Elastic scan along $[h,h,h]$ through $(\frac{1}{2},\frac{1}{2},\frac{1}{2})$, $(\overline{0.3},\overline{0.3},0.7)$, and $(0,0,1)$ under 0 T (blue) and 7 T (red) at 4 K. The region around $(\overline{0.3},\overline{0.3},0.7)$ is shown in the inset.

help us to distinguish between nuclear and magnetic scattering. The intensity was measured at a number of incommensurate peak positions in an unpolarized mode on SPINS and is compared to the square of the form factor, as shown in Fig. 1(b). The agreement again suggests that the incommensurate intensity is magnetic.

Previously, we showed that broad diffuse scattering develops at low temperatures around the (0,0,1) Bragg peak and attributed the intensity to ferromagnetic clusters.[12] Figure 1(c) shows that this signal, which is isolated by subtracting the 150 K data from the 4 K data, appears in both the SF and NSF channels. Note that because of the thermal expansion of the lattice constant and the presence of the strong nuclear Bragg peak in the NSF channel, there is a large wiggle in the subtracted NSF data very close to the peak center. The existence of SF scattering also confirms that this diffuse scattering has a magnetic component. The SF and NSF components have similar intensities which we expect for a sample that has domain-averaged ferromagnetic clusters.

### B. Scattering under applied field

ZFC and FC measurements were carried out to determine the field dependence of the commensurate and incommensurate features. The sample was initially cooled to 4 K in zero field and then an elastic scattering measurement (shown in blue in Fig. 2) was made along the $[h,h,h]$ direction in zero field through the (0,0,1) Bragg reflection. The sample was warmed up above $T_c$ and then field cooled under 7 T; the identical elastic scan was repeated at 7 T and 4 K (shown in red in Fig. 2). In these measurements, peaks were observed around three separate positions in reciprocal space: (i) $(\frac{1}{2},\frac{1}{2},\frac{1}{2})$, which arises from the $(\overline{1},\overline{1},1)$ Bragg reflection for neutrons of half the desired incident wavelength; (ii) $(\overline{0.3},\overline{0.3},0.7)$, which is the incommensurate peak; and (iii) (0,0,1), which has both nuclear and magnetic components, as discussed in Sec. III A. It is clear that the incommensurate peak intensity is significantly reduced in the applied field (see inset). We also observe that, if instead of field cooling, the magnetic field is applied after zero-field cooling, the incommensurate peak also decreases but slightly less dramatically, suggesting that the incommensurate order is affected by the thermal and magnetic history of the sample, which is not surprising considering the glassy features of the bulk susceptibility data.[10] The integrated incommensurate peak intensity as a function of the applied field is shown in Fig. 3, where it can be seen that the intensity drops continuously with the field.

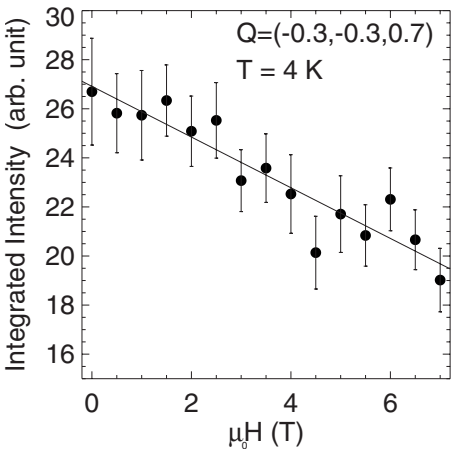


FIG. 3. The integrated satellite peak intensity versus applied field at 4 K. The solid line is a guide to the eye.

In an effort to determine what effect the applied field has on the ordering temperature for the incommensurate modulation, the order parameter of the incommensurate peak was measured upon warming in zero field after zero-field cooling and also upon warming in 7 T after field cooling in 7 T by a measurement of the intensity at $\vec{Q}=(\overline{0.32},\overline{0.32},0.68)$ as a function of temperature, as shown in Fig. 4. With field, the absolute intensity of scattering is reduced. The $Q$ scan along $[h,h,h]$ through the incommensurate peak under an applied field was also repeated at 50 K in order to determine if the field effect is more pronounced at a temperature closer to $T_{IC}$, as shown in the left panel of Fig. 5 (the 0 T data are ZFC, while the 7 T data are FC). A similar reduction in intensity as that at 4 K (Fig. 2) was observed. The scans were again repeated at 120 K in both 0 and 7 T to verify that there was no incommensurate scattering at that temperature, as shown in the right panel of Fig. 5.

We now consider the behavior of the broad ferromagnetic scattering under applied field. It is evident from the scans in Fig. 2 that the ferromagnetic scattering around (0,0,1) nar-

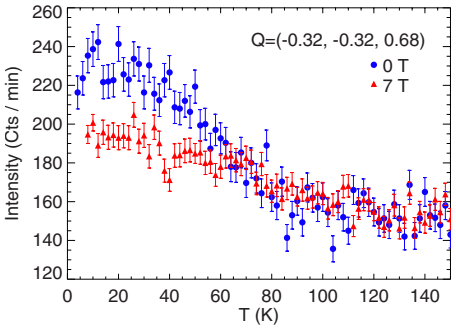


FIG. 4. (Color online) Temperature dependence of the incommensurate peak as measured at $\vec{Q}=(-0.32,-0.32,0.68)$ (Ref. 17) in 0 and 7 T.

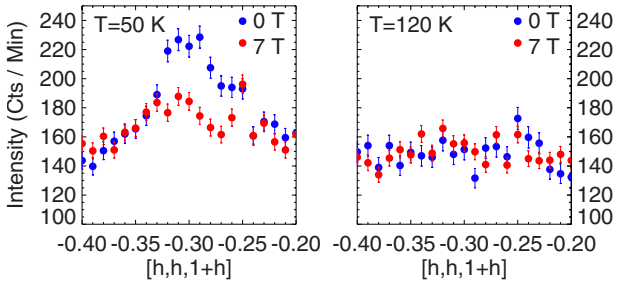


FIG. 5. (Color online) $Q$ scan along $[h,h,1+h]$ through the incommensurate peak at 50 K (left panel) and at 120 K (right panel) under 0 T (ZFC) and 7 T (FC).

rows considerably and significantly increases in field. This effect was further investigated by measuring the intensity along the longitudinal $[0,0,l]$ direction through the (0,0,1) Bragg peak in a two-axis mode. The sample was cooled in zero field, and then measurements were made as the field was increased, shown in Fig. 6(a), and again as the field was lowered, shown in Fig. 6(b). The intensity narrows and increases by more than an order of magnitude around the (0,0,1) Bragg reflection when the field is increased to 7 T. There is clearly a hysteretic effect, as the scans with increasing field differ from those with reducing field. Most notably, the intensity at (0,0,1) at 1 and 0 T was stronger after the field had already been ramped up to 7 T.

The intensity at (0,0,1) in zero field is expected to consist of a nuclear Bragg peak, with a Gaussian line shape, and a broad magnetic peak, which has a Lorentzian line shape.[12] The data were fitted at each field, upon ramping up and down, with a Gaussian, a Lorentzian, and a sloped background. We note that the higher angle shoulder of (0,0,1) appears in all of the scans in Fig. 6. The same scans along the longitudinal direction using NG1, which has better $Q$ resolution than BT9, did not reveal such a shoulder nor did our previous measurements on the SPINS spectrometer, which suggests it might be spurious or might be a second crystallite that is picked up in the current measurement due to a courser resolution. A second Gaussian function was included in the fits in order to describe the contribution from the shoulder, and the amplitude, FWHM, and position of the second Gaussian were fixed for all fields.[15]

Surprisingly, with the field on, it is not possible to describe the magnetic intensity only by a Lorentzian; instead,

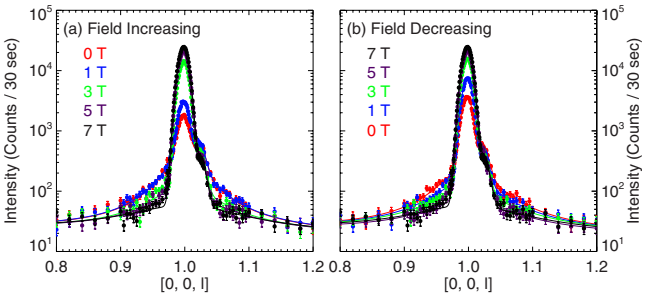


FIG. 6. (Color online) Diffraction measurements made in two-axis mode along the $[0,0,l]$ direction surrounding the (0,0,1) Bragg peak, shown in (a) with the field increasing and in (b) with the field decreasing.

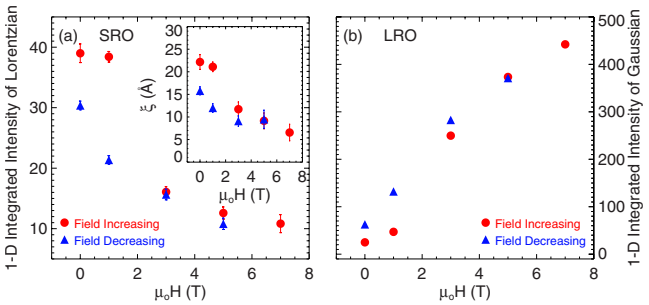


FIG. 7. (Color online) Evolution of the integrated intensity corresponding to the one-dimensional (1D) fitted Lorentzian component, shown in (a), and the 1D fitted Gaussian component, shown in (b), with increasing and decreasing field. The estimated correlation length associated with the Lorentzian component is shown in the inset of (a).

the amplitude of the Gaussian function increases considerably under the applied field, indicating that the magnetic intensity is a superposition of a Lorentzian and a Gaussian. The Gaussian component of the magnetic intensity describes regions of long-range order (LRO), which corresponds to correlations on a length scale longer than ~70 Å in the current configuration, whereas the Lorentzian components describe the broader diffuse intensity, which arises from regions of short-range order (SRO). The evolution of the integrated peak areas of the magnetic regions corresponding to the Gaussian and Lorentzian components (LRO and SRO) are shown in Figs. 7(a) and 7(b), respectively. Note that the nuclear contribution to the (0,0,1) Bragg peak is included in the integrated Gaussian intensity, so all values in Fig. 7(b) are offset by a constant nuclear contribution. The two components behave quite differently under applied field. As the field is increased, the LRO component increases dramatically, indicating that the volume fraction of LRO increases under the applied field, whereas the SRO component decreases and the volume fraction of SRO decreases. When the field is reduced, the LRO component decreases; yet a hysteretic effect is apparent at 3 T and below where the data points diverge from those measured as the field was initially increased, indicating that some remnant LRO appears to persist even in 0 T which did not exist prior to the initial application of the field. Similarly, when the field is reduced, the SRO component increases; however, the hysteresis is apparent since the initial amplitude of the SRO component does not completely recover the same value that was initially observed before the field was turned on. The correlation length of the SRO component, as determined by the inverse of the half-width at half maximum of the Lorentzian, is shown in the inset of Fig. 7(a), which suggests that the size of the SRO component actually decreases as the field is increased. This reduced correlation length may reflect the size of isolated ferromagnetic clusters that are unable to form larger entities under the applied field or it might be a side effect of the mixing of Lorentzian and Gaussian components during the fit.

From the data in Fig. 7, one can see that the total intensity measured in the cuts along $[0,0,l]$ increases as a function of field. It is important to note, however, that this does not

necessarily mean that the total volume fraction (SRO +LRO) of ferromagnetically correlated spins increases for it is actually the total ferromagnetic intensity integrated over a three-dimensional (3D) volume in reciprocal space that must increase if the volume fraction changes. To estimate the progression of the 3D integrated ferromagnetic intensity surrounding (0,0,1) under applied field, the cut along $[0,0,l]$ was numerically integrated over a spherical volume of radius 0.28 rlu surrounding (0,0,1) under the assumption that the scattering was spherically symmetric (the radius of 0.28 rlu was judged to be large enough because at that distance from the Bragg peak the intensity at 7 and 0 T was the same), and it was found that the integral did not change as a function of field. This was quite surprising because even in the absence of a change in the ferromagnetic volume fraction we expected to observe an enhancement due to alignment of spin polarizations of the different domains along the applied field and thus perpendicular to $\vec{Q}$. This is because ferromagnetic scattering intensity is proportional to the quantity $[1-(\hat{Q}\cdot\hat{n})^2]$, where $\hat{n}$ is a unit vector in the direction of spin polarization of a domain. Caciuffo *et al.*[16] determined that the domains are spin polarized along the (1,1,0) cubic axes, so if there is an equal population of the twelve (1,1,0)-type domains in zero field, then the ferromagnetic intensity at (0,0,1) should be increased by 50% when all domains become polarized perpendicular to $\vec{Q}$ by an applied magnetic field. Since we did not observe this effect even partially, we have to conclude that we cannot accurately estimate the 3D integrated intensity from only a cut along $[0,0,l]$. One possible reason could be that under the applied field the scattering becomes anisotropically distributed so that the assumption of spherically symmetric scattering fails; at any rate, we cannot make a conclusion regarding a change in the total ferromagnetic volume fraction under applied field.

In summary, our measurements of the $Q$ dependence of the incommensurate peaks and of the spin-polarized scattering clearly establishes the dominantly magnetic nature of both the incommensurate satellite peaks and the broad intensity surrounding (0,0,1) at low temperature. Our field measurements show that the incommensurate signal in the $(h,h,l)$ scattering plane progressively decreased with applied field. Either the incommensurate signal is destroyed by the application of the magnetic field or potentially the signal could be pushed out of the scattering plane along the direction of the applied field; experiments performed in a strong horizontal magnetic field could provide potentially useful information in this regard. As the field increases, giant ferromagnetic spin clusters form at the expense of smaller clusters.

## ACKNOWLEDGMENTS

The authors would like to acknowledge fruitful discussions with C. Leighton and thank him for discussing his unpublished data. They would also like to thank W. Ratcliff, C. F. Majkrzak, and B. J. Kirby of the NCNR for their assistance in the neutron scattering experiments and S. McKinney, E. Fitzgerald, and D. Dender of the NCNR for their assistance operating the superconducting magnet. This work is supported by the U.S. Department of Energy under Contracts No. DE-FG02-01ER45927 and No. DE-AC02-06CH11357, and the U.S. DOC through Contract No. NIST-70NANB5H1152. The use of the neutron scattering facilities at NIST was supported in part through NSF Grants No. DMR-9986442 and No. DMR-0086210.

[1] A. Moreo, S. Yunoki, and E. Dagotto, Science **283**, 2034 (1999).
[2] C. N. R. Rao, A. Arulraj, A. K. Cheetham, and B. Raveau, J. Phys.: Condens. Matter **12**, R83 (2000).
[3] E. Dagotto, Science **309**, 257 (2005).
[4] G. C. Milward, M. J. Calderon, and P. B. Littlewood, Nature (London) **433**, 607 (2005).
[5] M. J. R. Hoch, P. L. Kuhns, W. G. Moulton, A. P. Reyes, J. Wu, and C. Leighton, Phys. Rev. B **69**, 014425 (2004).
[6] P. L. Kuhns, M. J. R. Hoch, W. G. Moulton, A. P. Reyes, J. Wu, and C. Leighton, Phys. Rev. Lett. **91**, 127202 (2003).
[7] M. J. R. Hoch, P. L. Kuhns, W. G. Moulton, A. P. Reyes, J. Lu, J. Wu, and C. Leighton, Phys. Rev. B **70**, 174443 (2004).
[8] J. Wu, J. W. Lynn, C. J. Glinka, J. Burley, H. Zheng, J. F. Mitchell, and C. Leighton, Phys. Rev. Lett. **94**, 037201 (2005).
[9] D. Phelan, D. Louca, K. Kamazawa, S. H. Lee, S. Rosenkranz, M. F. Hundley, J. F. Mitchell, Y. Motome, S. N. Ancona, and Y. Moritomo, Phys. Rev. Lett. **97**, 235501 (2006).
[10] M. Itoh, I. Natori, S. Kubota, and K. Motoya, J. Phys. Soc. Jpn. **63**, 1486 (1994).
[11] J. Wu and C. Leighton, Phys. Rev. B **67**, 174408 (2003).
[12] D. Phelan, D. Louca, S. Rosenkranz, S. H. Lee, Y. Qiu, P. J. Chupas, R. Osborn, H. Zheng, J. F. Mitchell, J. R. D. Copley *et al.*, Phys. Rev. Lett. **96**, 027201 (2006).
[13] C. Leighton, American Conference on Neutron Scattering, Santa Fe, NM, USA, 2008 (unpublished).
[14] R. M. Moon, T. Riste, and W. C. Koehler, Phys. Rev. **181**, 920 (1969).
[15] In the following discussion, the use of the term "Gaussian" refers to the first Gaussian at (0,0,1) and not the Gaussian describing the shoulder.
[16] R. Caciuffo, D. Rinaldi, G. Barucca, J. Mira, J. Rivas, M. A. Senaris-Rodriguez, P. G. Radaelli, D. Fiorani, and J. B. Goodenough, Phys. Rev. B **59**, 1068 (1999).
[17] The incommensurate peak is broad enough that we expect no relevant difference between a measurement of the temperature dependence at $Q=(-0.32,-0.32,0.68)$ and $Q=(-0.3,-0.3,0.7)$.